Project closing report Katalin Burián (OTKA PD10442)

(2012-2014.)

I. Expression of Chlamydia muridarum plasmid genes and immunogenicity of pGP3 and pGP4 in different mouse strains.Mosolygó T, Faludi I, Balogh EP, Szabó ÁM, Karai A, Kerekes F, Virók DP, Endrész V, Burián K. *Int J Med Microbiol.* 2014 May;304(3-4):476-83. doi: 10.1016/j.ijmm.2014.02.005. Epub 2014 Feb 19.

The chlamydiae are obligate intracellular pathogens. Three species belong in the*Chlamydia* genus: *Chlamydia trachomatis*, the human pathogen.*C. trachomatis*, subdivided into two biovars clustering 18 serovars, is responsible for a broad spectrum of diseases worldwide. Serovars A, B, Ba and C of biovar trachoma infect the conjunctival epithelium and lead to ocular infections that can progress to trachoma, the leading cause of preventable blindness. The number of patients with trachoma is alarmingly high, and around a million of them are blind. Serovars D–K, which infect the genital epithelium and cause urogenital tract infections, remains the major aetiologic agents of sexually transmitted diseases in both developed and developing countries. Upper genital tract infections with *C. trachomatis* in women tend to have very serious consequences, including the onset of pelvic inflammatory disease. This syndrome often results in severe and irreversible sequelae, such as infertility or ectopic pregnancy

C. muridarum is a mouse-adapted strain and its genome exhibits high similarity to the *C. trachomatis* genome. Infection of mice with *C. muridarum* provides a useful model of the*C. trachomatis* infection in humans. Both Chlamydia species carry a highly-conserved plasmid with an approximate size of 7.5 kb. The plasmid o f *C. muridarum* (pMoPn) encodes seven open reading frames designated*TCA01–07*). *TCA04* and *TCA05* are known to encode the pGP3 and pGP4 proteins, respectively. It has been described that all plasmid-borne genes are transcribed and translated in the case of *C. trachomatis*. pGP3, one of the plasmid-encoded proteins, is secreted into the cytosol during *C. trachomatis*infection and has been found to be recognized by human antibodies. pGP3 elicits both humoral and mucosal immune responses in convalescent patients. The functions of the plasmid-encoded proteins in chlamydial pathogenesis or protective immunity are not known. Putative functions for several plasmid proteins have been assigned on the basis of homology to known proteins in the public databases (Thomas et al., 1997). One of the most intensely studied proteins, pGP3, has been implicated as a potential TLR4 agonist (Li et al., 2008). Naturally occurring plasmid-deficient clinical isolates are very rare and *in vivo* infection with plasmid-deficient strains is either asymptomatic (Kari et al., 2011) or accompanied by a significantly reduced pathology providing evidence that the plasmid plays an essential role in chlamydial pathogenesis. The primary purpose of the present study was to compare the levels of expression of different plasmid genes in genetically different BALB/c and C57BL/6N mice after pulmonary *C. muridarum* infection. Another aim was to monitor the immunogenicity of pGP3 and pGP4 encoded by pMoPn in different mouse strains. It has emerged that the expression of pMoPn genes and the immunogenicity of the examined plasmid proteins depend on the host genetic background.

Results

The kinetics of C. muridarum multiplication and the humoral immune response in BALB/c and C57BL/6N mice

The susceptibility of C57BL/6N and BALB/c mice to *C. muridarum* infection was investigated. Mice were infected intranasally with 1×10^3 IFU *C. muridarum* and sacrificed 1, 7, 14, 28 or 56 days after infection. From the first day after the infection, the BALB/c mice displayed more clinical symptoms than did the C57BL/6N mice, as indicated by ruffled fur, passivity, a lack of appetite and weight loss. The recoverable *C. muridarum* was determined by indirect immunofluorescence assay. In the BALB/c mice, the infectious *C. muridarum* titre was increased on day 1, peaked on day 7, and then decreased continuously. On day 28 after infection, the viable *C. muridarum* titre was 3×10^1 IFU/lung, but there was no detectable *C. muridarum* on day 56 after infection. In the C57BL/6N mice, the peak titre of *C. muridarum* was detected on day 7. By day 28 post-infection, all of the C57BL/6N mice were culture-negative, whereas all of the BALB/c mice remained culture-positive (Fig. 1)

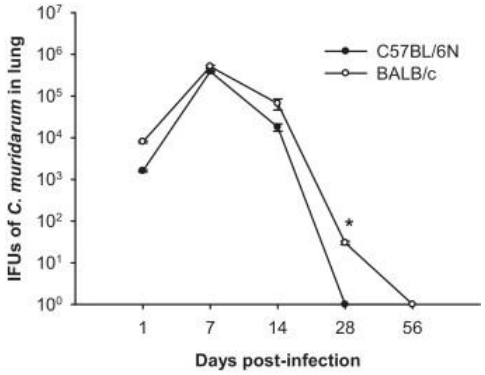

Fig. 1. *C. muridarum* IFUs in the lungs of *C. muridarum*-infected BALB/c and C57BL/6N mice

Expression of pMoPn genes in mice

Increased levels of expression of different plasmid genes were observed in the BALB/c mouse lungs on day 7 after infection. The expression of *TCA01*, *TCA02*, *TCA03*, *TCA06* and *TCA07* was 3–5-fold higher on day 7 relative to that in the control sample, and increased further to 5–7-fold on day 14. Interestingly, the increases in expression of *TCA04* and *TCA05* in the BALB/c mice were each 3-fold on both day 7 and day 14 (Fig. 2A). This result suggests that these two genes may be closely related. It was recently demonstrated bySong et al. (2013) that *Pgp4* is the protein that regulates the transcription of plasmid encoded *Pgp3* and multiple chromosomal genes during *Chlamydia trachomatis* infection. Moreover, a sequence of 30 or more nucleotides in the *Pgp3* gene was required for the optimal expression of *Pgp4* (Gong et al., 2013). In the C57BL/6N mice, the expression of the pMoPn genes was delayed. However, on day 14 the expression levels of the pMoPn genes in the C57BL/6N mice were higher (7–47-fold) than those in the BALB/c mice. There was no plasmid-encoded gene expression on day 28 after *C. muridarum* infection in either mouse strain.

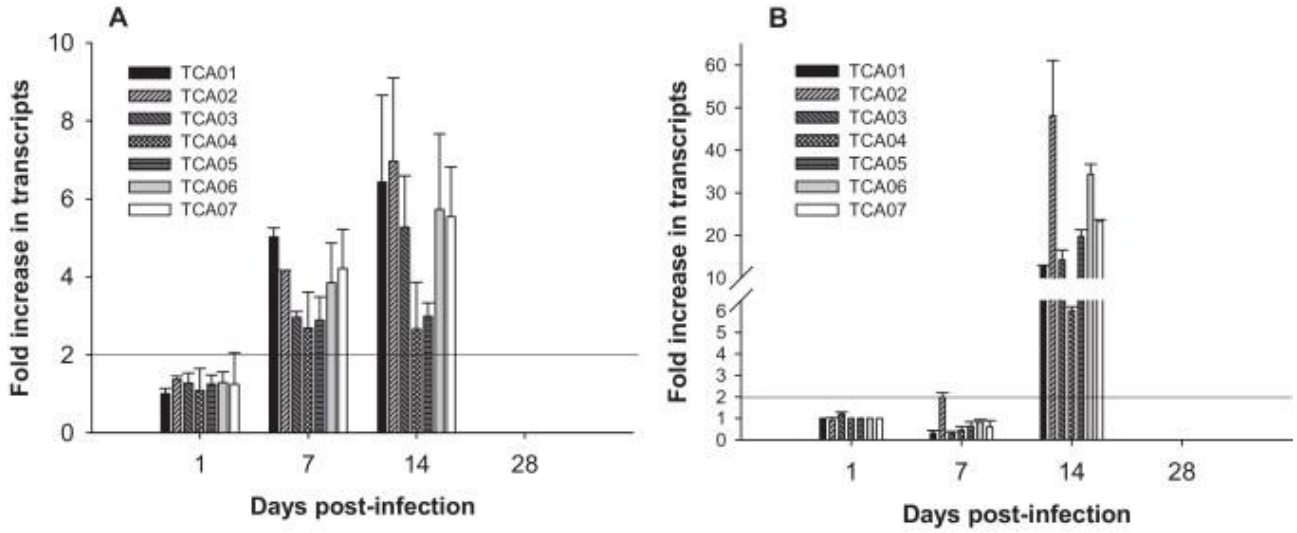

Fig. 2. Expression of different pMoPn genes in the lung suspensions of *C. muridarum*-infected BALB/c and C57BL/6N mice.

Production of pGP3- or pGP4-specific antibodies and identification of the proteins recognized byC. muridarum-infected BALB/c mice

During our experiment, the pGP4 protein was studied because its immunogenicity had not been checked earlier and its gene is found in close proximity to the TCA4 gene, and we hypothesized that pGP4 has an important role in the life of the pathogen. The pGP3 protein was used as a kind of positive control, because its role in the immune response after *C. trachomatis* infection was described earlier (Comanducci et al, 1994).

To clarify whether pGP3 and pGP4 are able to induce the production of specific antibodies or not in *C. muridarum*-infected mice, C57BL/6N and BALB/c mice were infected with *C. muridarum* 3 times at 4-week intervals. Groups of 10 mice were sacrificed at 2 weeks after each infection, sera were taken, and Western blot analysis was performed with the sera of the mice. Purified recombinant pGP3 or pGP4 protein or *C. muridarum* EBs served as antigens, and sera collected from uninfected mice were used as controls

In the C57BL/6N mice, a single infection with *C. muridarum* induced the production of pGP3-specific antibodies. No pGP4-specific antibody production was detected in mice infected once or twice but this antibody appeared after the 3rd inoculation (Fig. 3A). Moreover, serum samples of each *C. muridarum*-infected mouse reacted with the pGP4 protein (data not shown). The sera of the uninfected mice did not contain pGP3-, pGP4- or *C. muridarum*-specific antibodies. Sera of the *C. muridarum*-infected mice reacted with the lysate of concentrated *C. muridarum*. The sera of the *C. muridarum*-infected BALB/c mice did not react with the 28 kDa pGP3 and pGP4, but the sera of the singly or multiply infected BALB/c mice reacted with an additional protein with MW 80–85 kDa (Fig. 4A). The sera of the singly or multiply infected C57BL/6 mice did not show any reactivity with the trimeric form of pGP3 (Fig. 3B).

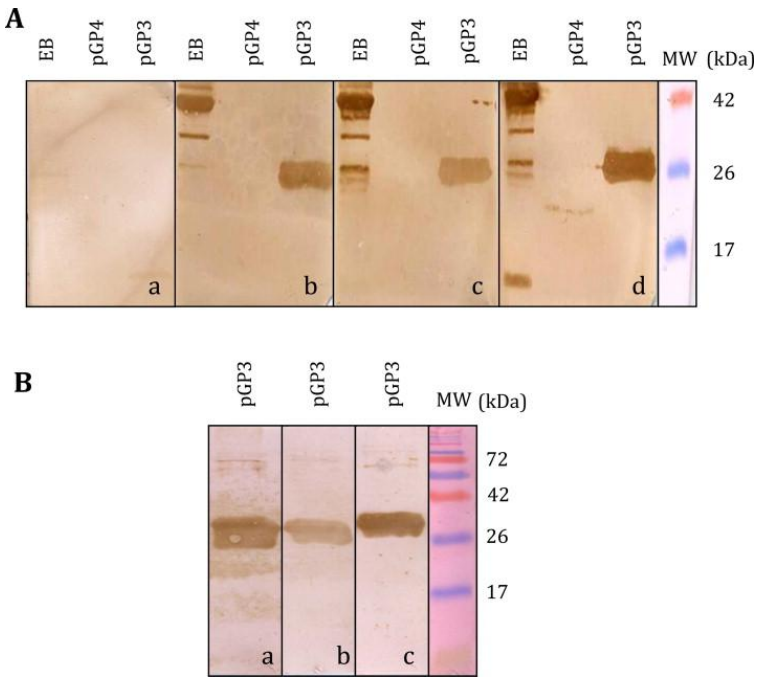

Fig. 3. Production of pGP3- and pGP4-specific antibodies in C57BL/6N mice infected 1–3 times with *C. muridarum* as tested in Western blot assays. (A) 2 µg of purified *C. muridarum* EBs or pGP4 or pGP3 recombinant protein were loaded onto a denaturing gel. After electrophoresis, the gel was blotted onto a PVDF membrane for Western blot detection with pooled sera of C57BL/6N mice infected 1 (panel b), 2 (panel c) or 3 times (panel d) with *C. muridarum*. A serum sample pooled from uninfected C57BL/6N mice was used as a negative control (panel a). (B) Pooled sera of C57BL/6N mice infected 1 (panel a), 2 (panel b) or 3 times (panel c) with *C. muridarum* did not react with the trimeric form of the pGP3 protein.

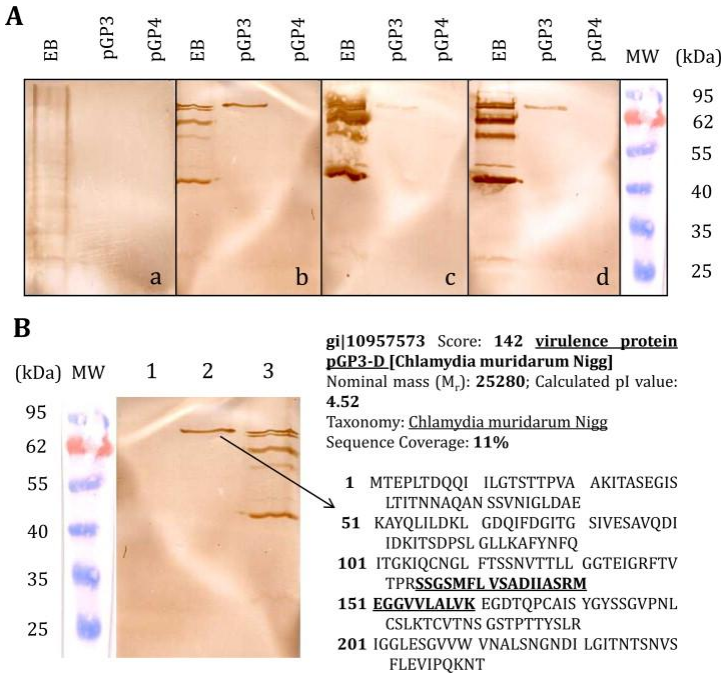

Fig. 4. Production of pGP3- and pGP4-specific antibodies in BALB/c mice infected 1–3 times with *C. muridarum* as tested in Western blot assays. (A) 2 µg of purified *C. muridarum* EBs or pGP3 or pGP4 recombinant proteins were loaded onto a denaturing gel. After electrophoresis, the gel was blotted onto a PVDF membrane for Western blot detection with pooled sera of BALB/c mice infected 1 (panel b), 2 (panel c) or

3 times (panel d) with *C. muridarum*. A serum sample pooled from uninfected BALB/c mice was used as a negative control (panel a). (B) Identification of the recombinant proteins. The gel slices containing the polypeptides of corresponding proteins which were recognized by the sera of *C. muridarum*-infected BALB/c mice in the blot assay were cut out from the gel and analysed by mass spectrometry on LC–MSMS instruments. The raw LC–MSMS data were converted into a Mascot generic file with Mascot Distiller software (v2.1.1.0). Acceptance criteria were at least 2 individual peptides with a minimum peptide score of 55 per protein. Peptide fragments that match the defined protein sequences are underlined.

As it was reported earlier that the pGP3 plasmid protein exists in trimeric or dimeric form (Chen et al., 2010), the samples corresponding to the trimeric pPG3 were subjected to further analysis. The result of the LC–MSMS experiment, which was confirmed by post source decay analysis, clearly showed that the protein which was recognized by the sera of the *C. muridarum*-infected BALB/c mice was the trimeric (84 kDa) form of pGP3 (Fig. 4B). The sera of the uninfected BALB/c mice did not react with the plasmid proteins or the *C. muridarum* EBs on Western blotting (Fig. 4A).

pGP3- and pGP4-specific cellular immune responses

For comparison and quantitation of the pGP3- and pGP4-specific T cell reactivity following *C. muridarum*infection in both mouse strains, lymphocyte proliferation assays were performed. The spleen cells of triply*C. muridarum*-infected mice, collected 2 weeks after the last infection, were re-stimulated in vitro with recombinant pGP3 or pGP4 proteins, heat-inactivated *C. muridarum* EBs or mock antigens. Uninfected mice served as controls. The spleen cells of the BALB/c mice did not show reactivity to the recombinant pGP4 protein after in vitro re-stimulation, but they recognized and responded with proliferation to the pGP3 protein after 72 h re-stimulation (Fig. 5A). The SIs were significantly higher after in vitro re-stimulation with pGP3 or pGP4 for 72 h in the *C. muridarum*-infected C57BL/6N mice than in the control group ($p < 0.05$) (Fig. 5B). Lymphocytes of both mouse strains reacted to heat-inactivated *C. muridarum* EBs with proliferation.

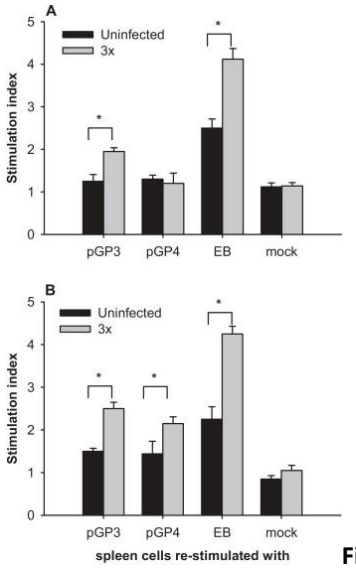

Fig. 5. pGP3- and pGP4-specific cellular immune response in triply *C. muridarum*-infected BALB/c and C57BL/6N mice, as tested in MTT tests. Spleen cells of mice collected 2 weeks after the last infection were re-stimulated in vitro with recombinant pGP3 or pGP4 protein; heat-inactivated *C. muridarum* EBs or mock antigens for 72 h. Uninfected mice served as controls. (A) Stimulation indices (SIs) of lymphocytes collected from infected and uninfected BALB/c mice. The data are the means ± standard deviation of the SIs of triplicate assays. *$p = 0.03$; $p < 0.001$. (B) SIs of lymphocytes collected from infected and

uninfected C57BL/6N mice. The data are the means ± standard deviation of the SIs of triplicate assays. *p = 0.012; p = 0.025; p = 0.02.

In summary, this study has demonstrated that the kinetics and the levels of change in the expression of the pMoPn genes depend on the genetic background of the host. The immune responses to the examined plasmid proteins also differed in the two mouse strains. pGP3- and pGP4-specific humoral and cellular immune responses were detected in C57BL/6N mice, but only a humoral response against the trimeric form of pGP3 in BALB/c mice after *C. muridarum* infection. Further experiments are needed to clarify the roles of pGP3 and pGP4 in the initiation of the cellular and humoral immune responses of the host in different mouse strains.

II. Protection promoted by pGP3 or pGP4 against Chlamydia muridarum is mediated by CD4(+) cells in C57BL/6N mice. Mosolygó T, Szabó AM, Balogh EP, Faludi I, Virók DP, Endrész V, Samu A, Krenács T, Burián K. *Vaccine.* 2014 Sep 8;32(40):5228-33. doi: 10.1016/j.vaccine.2014.07.039. Epub 2014 Jul 29.

In the present study, we set out to evaluate the efficacy of vaccination with recombinant pGP3 or pGP4 in the prevention of C. muridarum lung infection in a murine model. It emerged that multiple immunisation with pGP3 or pGP4 reduced the chlamydial burden and the inflammation in the lungs of mice after the challenge. Rather than the specific antibodies, it is the CD4+ lymphocytes that are responsible for the protective effect of the pGP3- or pGP4-specific immune response.

Results

Evaluation of the protective immunity of the pGP3 and pGP4 against C. muridarum infection

To reveal whether pGP3 or pGP4 can induce a protective immune response against *C. muridarum*, C57BL/6N mice were immunised subcutaneously 3 times at 3-week intervals with pGP3 or pGP4 mixed with Alum adjuvant. To determine the ability of the proteins to induce a humoral immune response, Western blot assay was carried out with sera obtained from immunised mice 2 weeks after the last immunisation. Purified pGP3, pGP4 or *C. muridarum* EBs served as antigens, and sera collected from Alum-immunised mice were used as controls. Multiple immunisation with pGP3 (Fig. 1, panel a) or pGP4 (Fig. 1, panel b) induced the production of protein-specific antibodies. The sera of the pGP3- or pGP4-immunised mice did not react with the whole EB lysate. The sera of Alum-immunised mice did not react with the recombinant pGP3, pGP4 or the whole *C. muridarum* (Fig. 1, panel c).

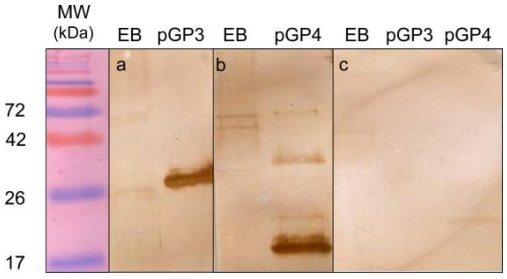

Fig. 1. Production of pGP3- or pGP4-specific antibodies in C57BL/6N mice immunised 3 times with pGP3 or pGP4, as tested by Western blot assay. Mice immunised with Alum alone served as controls. 2 μg of purified *C. muridarum* EBs or pGP3 or pGP4 was loaded onto a SDS-PAGE gel. After electrophoresis, the gel was blotted

onto a PVDF membrane for Western blot detection with sera of C57BL/6N mice immunised with pGP3 (panel a), pGP4 (panel b) or Alum alone (panel c).

Two weeks after the last immunisation, the mice were infected intranasally with *C. muridarum*, in order to explore whether the pGP3- or pGP4-specific immune response protected the mice against *C. muridarum*infection. On day 4 and 7 after infection, the body weight loss of the non-immunised mice was 8.5 ± 0.2% and 10.2 ± 0.3%, respectively, compared to the pGP3 and pGP4 immunised mice, the body weight of which did not change significantly after the infection (data not shown). The protective efficacy of pGP3 or pGP4 was determined by the *C. muridarum* burden in the lungs of mice (Fig. 2). Immunisation of the mice with the recombinant protein resulted in a significantly lower chlamydial load, irrespective of the protein used. The decrease observed in the case of pGP3 was approximately 1 log, while for pGP4 it was more than 1 log as compared with the control. Inflammatory infiltrates were significantly reduced in H&E stained lung sections of *C. muridarum*-infected mice immunised either with pGP3 (Fig. 3A) or pGP4 proteins (Fig. 3 B) compared to those of the controls (Fig. 3C). The alveolar structure can be clearly recognised in the lungs of immunised mice, compared to that of the control animals.

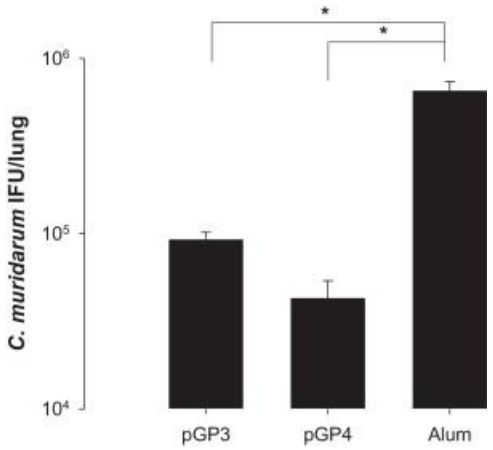

Fig. 2. *C. muridarum* titres in the lungs of pGP3- or pGP4-immunised mice after *C. muridarum* infection. Mice immunised with Alum alone were used as controls. Mice were infected with 2×10^3 IFU of *C. muridarum* 2 weeks after the last immunisation and then sacrificed 1 week later. Lung homogenates were inoculated onto McCoy cell monolayers, and chlamydial inclusions were detected by indirect immunofluorescence. Means ± standard deviations of *C. muridarum* titres (IFU/lung) in the lung homogenates from 10 individual mice in 3 independent experiments are shown. $^*p < 0.001$.

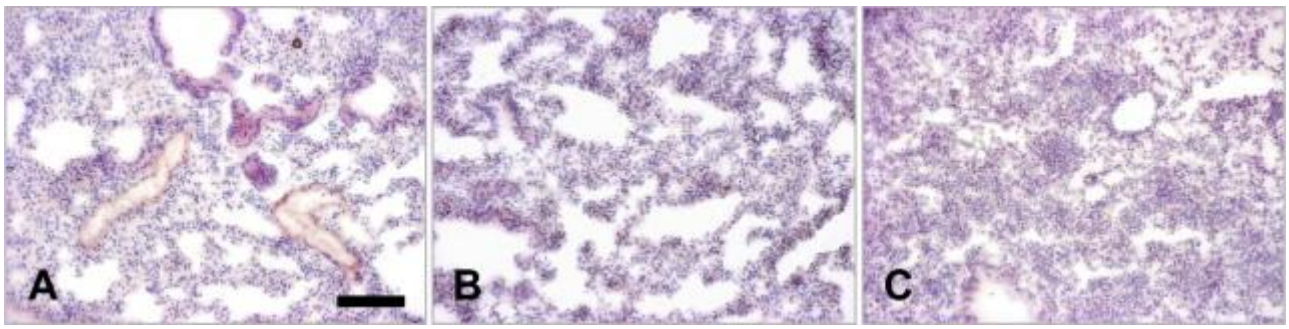

Fig. 3. Pathological changes of lung tissues observed by H&E staining. Lungs of control (C), pGP3- (A) or pGP4-immunised mice (B) were sectioned and stained with H&E 7 days after infection with *C. muridarum*. Mice immunised with Alum alone were used as controls.

A possible vaccine candidate must satisfy two criteria: induction of a protective immune response without the stimulation of pathological immunity during infection. In order to evaluate the augmentation of the inflammation after *C. muridarum* infection, we applied ELISA to determine the concentrations of IL-4, IL-10, IL-12 and IFN-γ in the lungs of immunised or control mice (Fig. 4). There were no significant differences in the levels of IL-4, IL-10 or IL-12 between the protein-immunised and control mice. However, the level of IFN-γ was significantly lower in the lungs of the immunised mice than in those of the control mice.

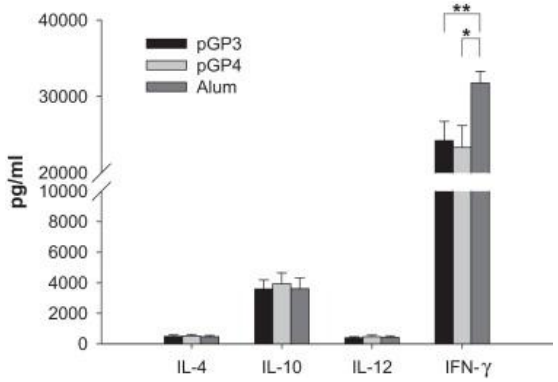

Fig. 4. Production of inflammatory cytokines in the lungs of mice immunised with pGP3 or pGP4 protein or Alum alone. Lung homogenates were tested by using an IL-4, IL-10, IL-12 and IFN-γ ELISA kit according to the manufacturer's instructions. The data are means ± standard deviations of the results obtained on 10 mouse lungs in 3 independent experiments. $^{*}p = 0.004$; $^{**}p = 0.011$.

Effect of passive immunisation with pGP3- or pGP4-specific antibodies and spleen cells of immunised mice on the outcome of C. muridarum infection

As the immunisation with pGP3 or pGP4 elicited specific antibody responses, we next assessed the capacity of the antibodies to protect against *C. muridarum* infection. For the *in vivo* neutralisation of *C. muridarum*, sera of pGP3-, pGP4-immunised or control mice were collected 2 weeks after the last immunisation and administered to naive mice before and after *C. muridarum* infection. The mice were sacrificed 1 week after the infection; the recoverable chlamydiae in the lungs were determined. The titre of viable *C. muridarum* was not significantly lower in the lungs of the mice treated with the immune serum as compared with that in the control mice (Fig. 5). To test the infectivity of *in vitro* antibody-treated *C. muridarum*, naive mice were infected with *C. muridarum* EBs incubated *in vitro* with sera of immunised or control mice. The sera of the immunised mice did not contain antibodies which were able to provide protection against *C. muridarum* and decrease the bacterial burden in the lungs of mice (Fig. 5).

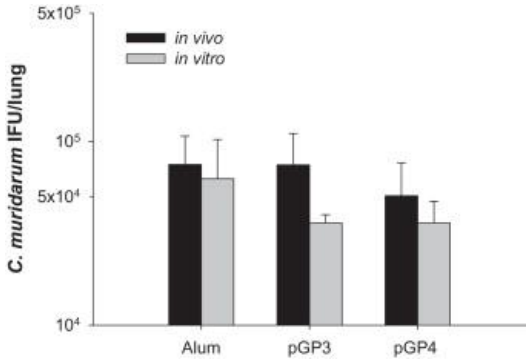

Fig. 5. *In vivo* and *in vitro* neutralisation of *C. muridarum* with sera of pGP3-, pGP4-immunised or control mice. Naive mice were treated *in vivo* with the sera of immunised or control mice before and after *C. muridarum* infection or were infected with *C. muridarum*treated *in vitro* with sera obtained from immunised or control mice. Sera from mice treated with Alum alone were used as controls. The chlamydial burden in the lungs of mice was determined by indirect immunofluorescence test 1 week after the infection. Means ± standard deviation of *C. muridarum* titres (IFU/lung) in the lung homogenates from 10 individual mice in 3 independent experiments is shown.

Since we did not demonstrate antibodies with neutralising activity in mice immunised with pGP3 or pGP4, we investigated the protective effect of the pGP3- and pGP4-specific cellular immune response. Spleen cells of immunised or control mice depleted of $CD4^+$ or $CD8^+$ cells were transferred to naive mice. 24 h after the adoptive transfer, the mice were infected with *C. muridarum*. The adoptive transfer of pGP3- or pGP4-specific spleen cells depleted of $CD8^+$ cells significantly reduced the chlamydial load in the lungs of mice as compared with the control (Fig. 6). Adoptive transfer with spleen cells depleted with the anti-CD4 monoclonal antibody did not give rise to a significant reduction in the chlamydial burden.

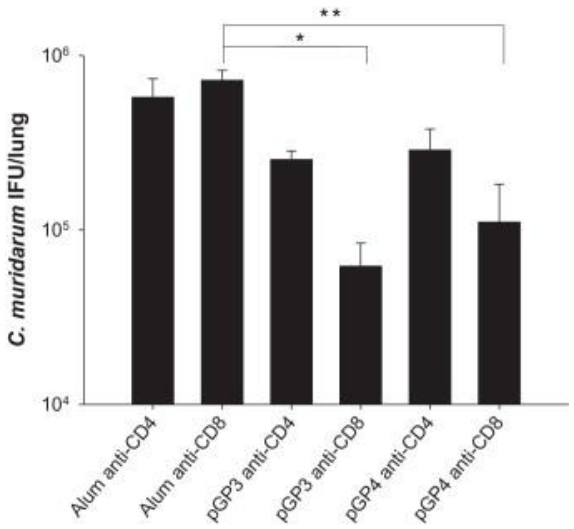

Fig. 6. The chlamydial load in the lungs following the adoptive transfer of spleen cells. Groups of 10 mice were treated with spleen cells depleted of $CD4^+$ or $CD8^+$ cells, obtained from pGP3- or pGP4-immunised mice. Naive mice transferred with spleen cells collected from Alum-treated mice were used as controls. One day after the adoptive transfer, the mice were infected with *C. muridarum*, and 1 week later they were sacrificed and the recoverable chlamydiae were detected by indirect immunofluorescence test. The means ± standard deviation of *C. muridarum* titres (IFU/lung) in the lung homogenates from 10 individual mice in 3 independent experiments is shown. $^*p = 0.029$; $^{**}p < 0.001$.

Multiple immunisation with pGP3 led to a significantly reduced chlamydial burden in the lungs of mice after the challenge. It is a new finding that immunisation with the regulatory pGP4 can elicit protection similar to that with pGP3. It is not the pGP3- or pGP4-specific antibodies but rather the specific $CD4^+$ cells that are responsible for the protective effect of the immune response against *C. muridarum* infection. These results provide important information for future studies of vaccine development against chlamydial infections.

III. IL-17E production is elevated in the lungs of Balb/c mice in the later stages of Chlamydia muridarum infection and re-infection. Mosolygó T, Spengler G, Endrész V, Laczi K, Perei K, Burián K. *In Vivo*. 2013 Nov-Dec;27(6):787-92.

IL-17 cytokines can aggravate the pathogenesis of autoimmune diseases, but they have a beneficial role during infection caused by different pathogens (Iwakura et al, 2008). The role of IL-17E in respiratory diseases, and particularly in re-infections, has not been elucidated. The role of pathogens in the development and reactivations of asthma is an exciting field, but the exact pathomechanism is not known. We recently reported that the re-infection of mice with *C. pneumoniae* can induce a high level of IL-17E four weeks after infection, which indicates that IL-17E induced by reinfection with *C. pneumoniae* possibly influences allergic/asthmatic diseases (Mosolygó et al , 2013). In the present article, we wished to demonstrate that infection with another pathogen can also induce the production of IL-17E, which plays an important part in allergic asthma by promoting the release of Th2 cytokines such as IL-4, IL-5 and IL-13.

Results

C. muridarum infection and re-infection induce the expression of IL-17A and IL-17E mRNA in the lungs of mice. To investigate the production of IL-17A and IL-17E cytokines during *C. muridarum* infection, Balb/c mice were infected intranasally with *C. muridarum*, and subsequently reinfected on day 28 after the first infection. On days 1, 7, 14,28, 29, 35, 42 and 56 after the first infection, groups of seven mice were sacrificed and their lungs were collected for the determination of *C. muridarum* titres, mRNA levels and protein contents of the IL-17A and IL-17E cytokines in individual lungs. The recoverable *C. muridarum* was determined by indirect immunofluorescence assay. The infectious *C. muridarum* titre in the mice increased to 8.25×103 IFU/lung by day 1, peaked at 5.23×105 IFU/lung on day 7, and then decreased to 3×101 IFU/lung by day 28 after infection. On day 29, one day after the re-infection the bacterial titre was 5.25×103 IFU/lung but at later time points, viable *C. muridarum* was not detected in the lungs of the reinfected mice (Figure 1).

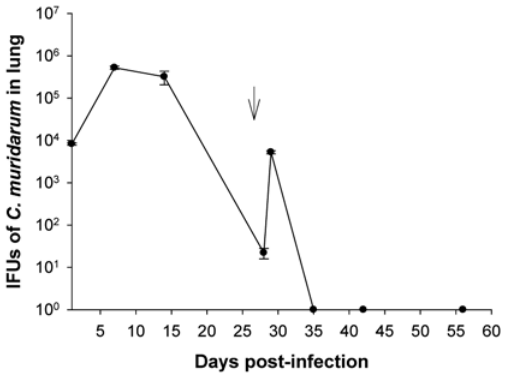

Figure 1. *Chlamydia muridarum* inclusion forming unit (IFU) levels in the lungs of *C. muridarum*-infected and re-infected mice.

The expression of *IL-17A* mRNA was highest (20-fold) on day 7, and then decreased continuously. The expression of *IL- 17A* mRNA after re-infection displayed similar kinetics as after the primary infection, but the fold increases in transcripts were higher: 30-, 90- and 40-fold on day 29, 35 and 42, respectively (Figure 2a). The kinetics of IL-17A protein production correlated with the mRNA production increased from day 1, with the highest concentration observed on day 7 (Figure 2b).

Unlike that of *IL-17A* mRNA, the expression of *IL-17E* mRNA did not demonstrate a parallel with the bacterial burden in the lungs of the mice. The expression started to increase on day 7, and the highest level (860-fold) was detected on day 28 after the first infection. On day 29 (one day after re-infection), the expression of *IL-17E* mRNA decreased dramatically, but after that it increased again and was highest (1600-fold) 28 days after re-infection, when the experiment was terminated (Figure 2a). The kinetics of IL-17E protein production was similar to that of the expression of *IL-17E* mRNA in the lungs of the infected and the re-infected mice (Figure 2b).

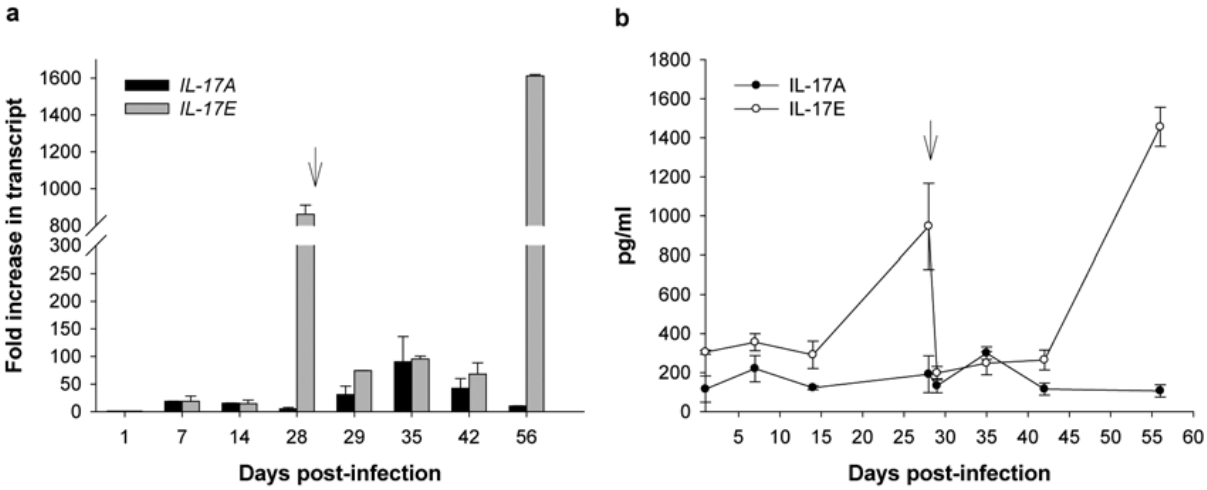

Figure 2. : Expression of interleukin 17A (IL-17A) and IL-17E mRNA in lung suspensions from *Chlamydia muridarum*-infected and re-infected mice.

The production of IL-17E is compartmentalized. IL-17E is known to be produced by different cell types, *e.g.* Tlymphocytesand epithelial cells (16). However, it was notclear which cells are responsible for the production of IL-17E after *C. muridarum* infection. To investigate whether there is an increase in IL-17E level at the periphery, a lymphocyte proliferation assay was carried out. Spleen cells from mice which had been infected once or twice and killed two or four weeks after infection and re-infection, were re-stimulated with a mock preparation, or live or heat-inactivated *C. muridarum*, or left unstimulated. Spleen cells from uninfected mice served as controls. The IL-17A and IL-17E cytokines were measured by ELISA. There was no detectable IL-17E production in the supernatants of the re-stimulated or unstimulated spleen cells collected from *C. muridarum*-infected and uninfected mice. The quantity of IL-17A was also not increased in the supernatants of the spleen cells isolated from uninfected mice or of the spleen cells left unstimulated (data not shown). In contrast, the spleen cells from infected or re-infected mice produced IL-17A after *in vitro* re-stimulation with viable or heat-inactivated *C. muridarum*. There were no significant differences in IL-17A production between the spleen cells re-stimulated with viable or heat-inactivated *C. muridarum*. The quantity of the IL-17A cytokine produced by the spleen cells was lower in the mice which had been infected in vivo with *C. muridarum* only once, independently of the stimulation conditions (Figure 3).

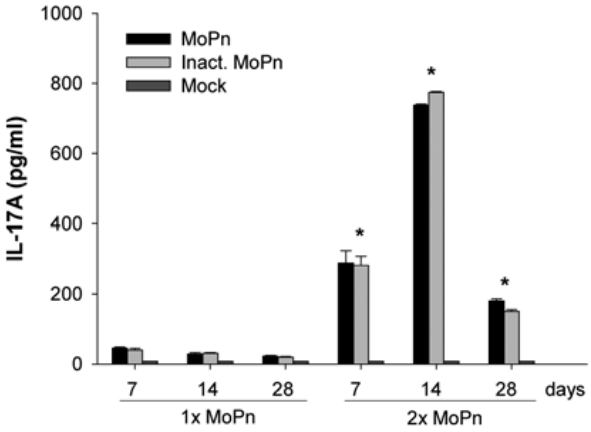

Figure 3. The interleukin 17A (IL-17A) production of the spleen cells isolated from infected (1× MoPn) and re-infected (2× MoPn) mice.

To investigate IL-17E-producing cells further, the lungs of infected, re-infected and uninfected mice were sectioned and stained with monoclonal antibody to IL-17E as primary, and FITC-labelled anti-mouse IgG as a secondary antibody. No fluorescence was seen in the lung sections of the uninfected mice (Figure 4a). The production of IL-17E was observed in the lungs of the infected and re-infected mice four weeks after infection. The IL-17E-positive cells were situated especially among the epithelial cells of the bronchi, and only a few positive cells were found in the interstitium of the lungs (Figure 4b and c).

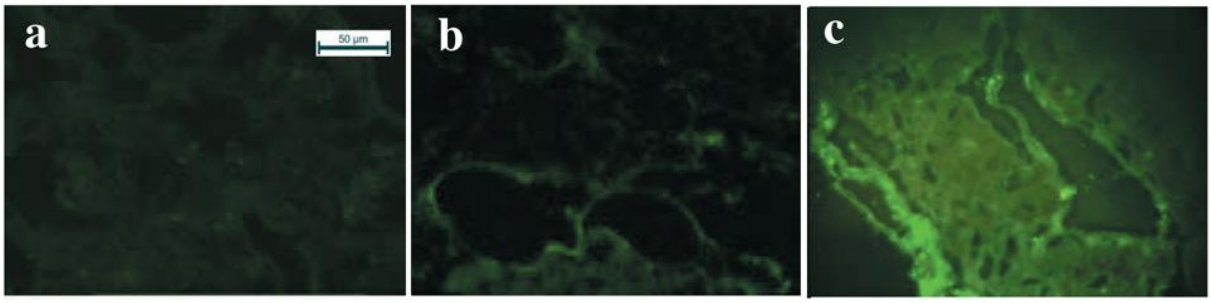

Figure 4. The production of interleukin 17E (IL-17E) in the lungs of uninfected (a), *Chlamydia muridarum*-infected (b) and re-infected mice (c). The lung sections were stained with IL-17E-specific monoclonal antibody and with fluorescein isothiocyanate (FITC)-labelled anti-mouse IgG.

In the present work, we demonstrate that *C. muridarum* infection and re-infection induce the expression of IL-17E at the mRNA and protein levels in the lungs of Balb/c mice inthe later stages of infection. The production of IL-17E iscompartmentalized, occurring in the epithelial cells around the bronchi. Multiple *C. muridarum* infectios- induced high amountof IL-17E production can play an important part in the pathogenesisof allergic pulmonary diseases.

IV. Anti-chlamydial effect of plant peptides.Balogh EP, Mosolygó T, Tiricz H, Szabó AM, Karai A, Kerekes , Virók DP, Kondorosi E, Burián K. *Acta Microbiol Immunol Hung*. 2014 Jun;61(2):229-39. doi: 10.1556/AMicr.61.2014.2.12

At the individual level, *C. trachomatis* infection can generally be treated effectively with antibiotics, though antibiotic resistance appears to be increasing [Shaw et al., 2011]. At the population level, public health control of the infection is rather problematic. With regard to the severe potential consequences of urogenital *C. trachomatis* infection in women, many countries offer screening.

Vaccination, which is currently unavailable, would be the best way to reduce the prevalence of *C. trachomatis* infections, as it would be much cheaper and would have a greater impact on controlling *C. trachomatis* infections worldwide [Schautteet et al., 2011]. The development of new antimicrobial agents is required to overcome this problem.

Antimicrobial peptides (AMPs), natural antibiotics produced by nearly all organisms, from bacteria to plants and animals, are crucial effectors of innate immune systems, with different spectra of antimicrobial activity and with the ability to perform rapid killing. To date, more than 800 AMPs have been discovered in various organisms, including 270 from plants. It has become clear in recent years that these peptides are able not only to kill a variety of pathogens, but also to modulate immune responses in mammals. However, their modes of action are poorly understood. In some species these peptides serve as the primary antimicrobial defense mechanism, whereas in others they serve as an adjunct to existing innate and adaptive immune systems [Brogden et al., 2003]. Cationic AMPs interact with negatively charged microbial membranes and permeabilize the membrane phospholipid bilayer, resulting in lysis and the death of microbes [Powers et al., 2003]. In view of their rapid and broadspectrum antimicrobial properties, interest has emerged in AMPs as potential antibiotic pharmaceuticals with which to combat infections and microbial drug resistance [Hadley et al., 2010].

Most plant AMPs are cysteine cluster proteins. This group includes major plant immunity effectors such as defensins, and also symbiotic peptides, including the nodule-specific cysteine rich (NCR) peptides, which are produced in *Medicago Sinorhizobium meliloti* symbiosis and provoke irreversible differentiation of the endosymbiont. The NCR family is composed of about 500 divergent peptides in *Medicago truncatula* [Nallu et al., 2011]. Some cationic NCRs have been shown to possess genuine antimicrobial activities *in vitro,* killing various Gram-negative and Gram-positive bacteria highly efficiently [Tiricz etal., 2013].

Results

Anti-chlamydial effect of plant peptides

To determine whether they possess anti-chlamydial activity, 11 NCR peptides (NCR030, NC0R44, NCR055, NCR095, NCR137, NCR168, NCR169, NCR183, NCR192, NCR247 and NCR280) were co-incubated individually with *C. trachomatis* EBs at 10 µg/ml for 2 h at 37°C. Counting of the number of viableC. trachomatis inclusions demonstrated that 7 of the 11 peptides (NCR044, NCR055, NCR095, NCR183, NCR192, NCR247 and NCR280) were effective killers of C. trachomatis in vitro, while NCR030 and NCR168 displayed weaker activity and NCR137 and NCR169 did not exert an anti-chlamydial effect (Fig.1A). C. trachomatis inclusions were then treated for 2 h with concentrations of the peptides ranging from 1.25 µg/ml to 10 µg/ml (Fig. 1B). NCR044, NCR055 and NCR183 were found to exert the strongest anti-chlamydial activities by reducing the viability to 95%, 78% and 85%, respectively, at 1.25 µg/ml, whereas the other peptides revealed no effect at 1.25 µg/ml concentration. NCR192 and NCR247 had significant anti-chlamydial effects at 2.5 µg/ml concentration. The time course of killing was investigated in the cases of NCR044, NCR055, NCR183 and NCR247 at 5 µg/ml concentration (Fig. 1C). NCR044 elicited the fastest effect, achieving an 80% reduction in the number of viable Chlamydia inclusions after a 15-min co-incubation with C. trachomatis EBs. The other three peptides required longer times to attain the killing effect. Of the tested peptides, therefore, NCR044 exhibited the strongest anti-chlamydial activity, acting at the lowest concentration and most rapidly.

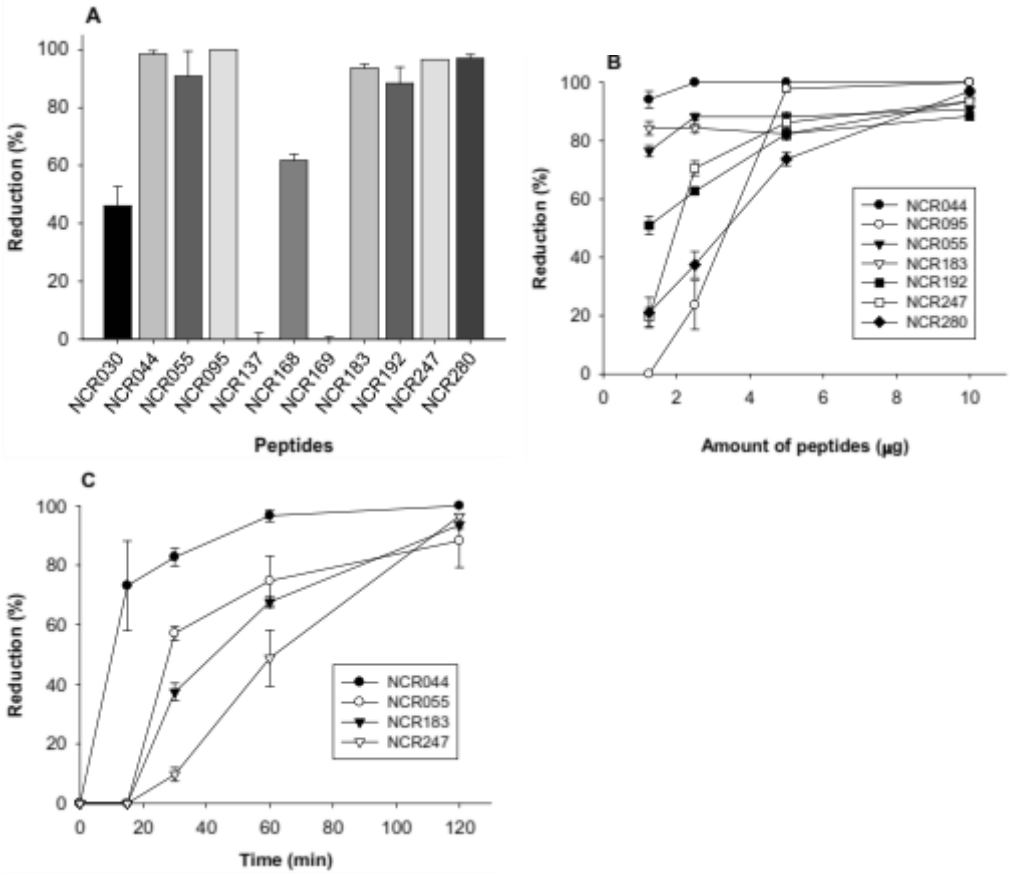

Figure 1. Concentration and time dependences of the anti-chlamydial effects of NCR peptides

Identification of the chlamydial ligand responsible for NCR247 binding

Further investigations were carried out with NCR247, which displayed anit-chlamydial activity in the previous tests. To identify the chlamydial ligand responsible for NCR peptide binding, concentrated C. trachomatis EB preparations and mock control preparations were separated by SDS-PAGE. After blotting, the membranes were probed with synthetic NCR247 peptide and incubated with anti-NCR247 IgG and then with HRP-labeled anti-rabbit antibody. The control lane with Chlamydia EBs was stained with anti-NCR247 IgG and HRP-labeled anti-rabbit antibody without incubation with synthetic NCR247 peptide. The synthetic NCR247 peptide was bound to a 60-kDa protein band in the Chlamydia lysate (Fig. 2A, lane 4). The synthetic NCR247 did not react with the mock lysate (lane 2), and the Chlamydia EB lysate did not react with the HRP-conjugated anti-rabbit antibody (lane 3). The gel slice containing the corresponding polypeptide of the concentrated C. trachomatis EBs associated with the synthetic NCR247 peptide was cut out from the gel and analyzed by LC-MSMS. A60 kDa putative GroEL protein of Chlamydia was indicated by LC-MSMS and confirmed by post source decay analysis (Fig. 2B).

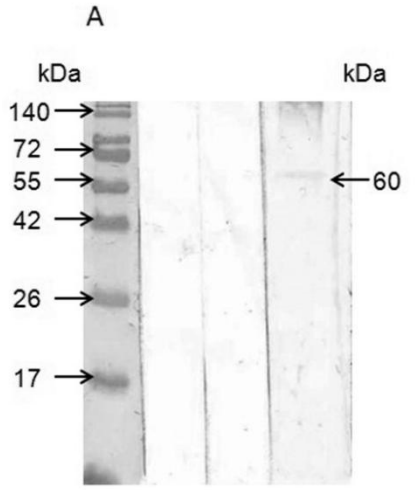

B

D7DCT1 Uniprot ID: D7DCT1_CHLTD Species: CHLTD Name: 60 kDa chaperonin
Organism: Chlamydia trachomatis serovar D (strain D-EC) Gene: groEL Existence: Inferred from homology Version: 1
Protein MW: 58147.4 Protein pI: 5.3 Protein Length: 544

Num Unique	% Cov	Best Disc Score	Best Expect Val
17	36.9	4.84	8.1e-8

m/z	z	Da	Peptide	RT	Start	End	Score	Expect
643.6846	3	0.040	EVELADKHENMGAQMVK	13.5501	59	75	18.6	0.015
615.7597	2	-0.051	NVTAGANPMDLK	15.3489	106	117	36.5	1.9e-5
911.0538	3	-0.066	EIAQVATISANNDAEIGNLIAEAM(Oxidation)EK	27.2683	143	168	26.1	7.9e-6
957.1231	3	-0.016	NGSITVEEAKGFETVLDIVEGMNFNR	35.3565	172	197	20.3	0.0027
928.9320	2	-0.014	GFETVLDIVEGM(Oxidation)NFNR	29.8399	182	197	46.0	2.4e-7
920.9175	2	-0.031	GFETVLDIVEGMNFNR	33.6069	182	197	49.1	8.1e-8
1122.8975	3	0.011	GYLSSYFATNPETQEC(Carbamidomethyl)VLEDALVLIYDKK	34.1365	198	226	22.8	1.6e-6
826.1337	3	0.028	KAM(Oxidation)LEDIAILTGGQLISEELGMK	31.5225	286	308	30.6	1.1e-6
820.7403	3	-0.034	KAMLEDIAILTGGQLISEELGMK	33.2856	286	308	37.2	4.5e-7
1173.6437	3	0.034	AM(Oxidation)LEDIAILTGGQLISEELGMKLENANLAM(Oxidation)LGK	35.7915	287	319	20.4	7.4e-4
1168.3364	3	0.058	AMLEDIAILTGGQLISEELGM(Oxidation)KLENANLAMLGK	37.7253	287	319	29.5	1.0e-6
1166.6025	2	-0.0081	AMLEDIAILTGGQLISEELGMK	36.0232	287	308	47.2	6.3e-7
595.2812	2	-0.035	LENANLAM(Oxidation)LGK	15.5306	309	319	34.9	4.2e-6
665.3198	3	0.0022	EDTTIVEGM(Oxidation)GEKEALEAR	14.4267	328	345	19.8	0.0080
763.8327	2	0.0044	Q(Gln->pyro-Glu)IEDSSSDYDKEK	11.5751	352	364	18.1	0.0078
524.7479	2	-0.023	VGAATEIEMK	13.1456	381	390	35.2	3.5e-5
861.8609	2	-0.055	DAYTDMLEAGILDPAK	27.4021	485	500	31.1	3.8e-4

Figure 2. Interaction of NCR247 peptide and *C. trachomatis* EBs. Far-Western blot analysis of the chlamydial ligands responsible for NCR247 peptide binding. (A) Identification of the *C. trachomatis* proteins by LC-MSMS (B). Peptide fragments that match the defined protein sequences are to be found in the table

FACS analysis for the detection of NCR247 binding to the whole C. trachomatis *EBs*

To show that NCR247 is able to bind not only to the degraded *Chlamydia* particles but to the native, viable *Chlamydia* EBs, a FACS analysis was carried out. Figure 3 reveals that *Chlamydia* EBs interacted with FITC-conjugated NCR247 peptide. Untreated or FITC-labeled NCR035 peptide-treated (this peptide showed no anti-chlamydial effect earlier) *Chlamydia* EBs did not demonstrate increased fluorescence.

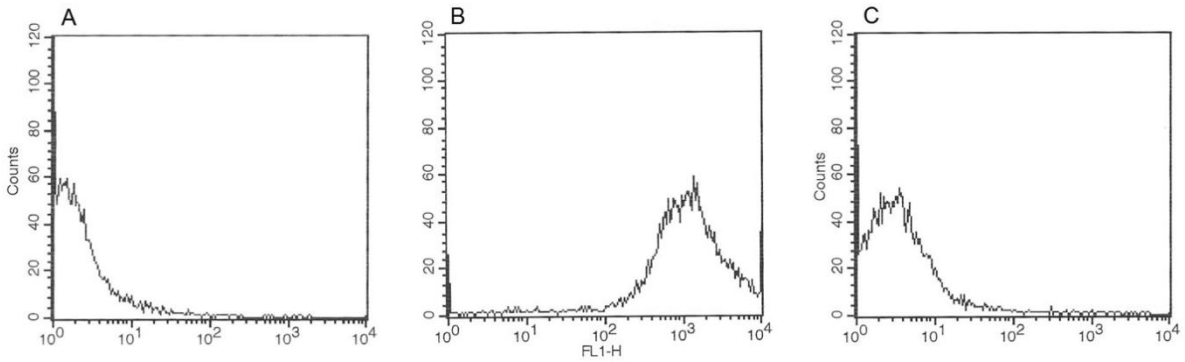

Figure 3. FACS analysis of NCR247 peptide binding to whole *C. trachomatis* EBs.

The present study indicates that certain of the NCR peptides possess substantial*in vitro* activity against *C. trachomatis* D. Studies of chlamydial infection in animal models are clearly needed to establish whether they have parallel *in vivo* results and whether these peptides can be useful lead compounds for the development of anti-chlamydial drugs

V. Application of DNA chip scanning technology for automatic detection of Chlamydia trachomatis and Chlamydia pneumoniae inclusions.Bogdanov A, Endrész V, Urbán S, Lantos I, Deák J, Burián K, Önder K, Ayaydin F, Balázs P, Virok DP.*Antimicrob Agents Chemother.* 2014;58(1):405-13. doi: 10.1128/AAC.01400-13. Epub 2013 Nov 4

The antibiotics used for therapy of chlamydia infections include tetracyclines and macrolides. While antibiotic therapy is effective in the majority of cases, tetracycline and azithromycin resistance has been reported (O'Neill et al., 2013).

Discovery of novel antimicrobial compounds for treatment and possible chemoprevention is a medically important research task. High-throughput testing of potentially antichlamydial compounds is hampered by the small size and obligate intracellular propagation of the bacterium. After infecting the host cell, the chlamydia propagates in a distinct cellular space called an inclusion. Since, at a low multiplicity of infection (MOI), one chlamydia can form one inclusion, the original chlamydia count is indirectly measured by labeling and manual microscopy counting of inclusions. To circumvent the labor-intensive and subjective manual counting, we designed a relatively low-cost, easy-to-use system that automatically counts chlamydial inclusions. The system consists of a commercial DNA chip scanner and custom-made image analysis software. DNA chip and microarray scanners are devices widely used for the high-resolution scanning of glass slides that contain a large number of DNA probes that bind fluorescently labeled cDNAs or DNAs. We applied this system to detect fluorescently labeled chlamydial inclusions in host cells propagated in a 16-well chamber slide. We designed ChlamyCount, a custom ImageJ plug-in for the completely automatic detection of fluorescently labeled chlamydial inclusions on the scanned image. ImageJ is a Java-based, platform-independent, freely available image analysis software package (Collins, 2007). ImageJ can be specifically tailored to a given application using user-made plug-ins. The image processing with ChlamyCount is almost fully automatic, including the extraction of the areas of the 16 wells, the automatic detection of inclusions in each well, dissection and counting of individual inclusions, and automatic reporting.

ChlamyCount software

McCoy epithelial cells grown on a 16-well chamber slide were used for chlamydial infection. Depending on the chlamydial strain, we removed the chamber at 24 or 48 h postinfection (p.i.), fixed the host cells, and stained the chlamydial inclusions with Cy5 analogue Alexa 647-labeled anti-chlamydial LPS antibody. The stained inclusions were scanned with a commercially available Axon GenePix 4100 DNA chip scanner. The scanner is capable of scanning Cy3- or Cy5-labeled spots on a regular microscope glass slide with a maximum resolution of 5 μm, which is comparable to the size of a chlamydial inclusion (Fig. 1A to D. The scanned image is processed by the ChlamyCount software. The thresholds for the minimum intensity and size of the inclusion are adjustable by the user; otherwise, preset threshold values are applied (Fig. 2A). The two threshold values are the only parameters that can be adjusted by the user; all the subsequent steps are automatic. If the user adjusts the intensity and/or area threshold, the effect of the adjustment can immediately be seen by a magnified quarter of the uppermost well and the well in the lowest left-hand side (Fig. 2B). In the next step, ChlamyCount automatically crops the 16 areas containing the host cells from the complete image. For each area, ChlamyCount processes the images as follows: (i) the pixels with low intensity values are likely noise; thus, they are eliminated by thresholding the image with an intensity and area threshold value; (ii) regions having an area greater than the median of the area of all regions (the suspected size of a single inclusion) are split by finding the local maxima in the regions and then assigning each point to the same closest maximum to form smaller regions; and (iii) the identified particles are encountered and their boundaries are determined. It is worth noting that the splitting of high-intensity areas is not complete; larger high-intensity areas likely to contain multiple infected

cells without clear boundaries between them are regarded as one particle (inclusion). On the other hand, this effect can be observed at both higher and lower MOIs; therefore, the correlation of detected particles with the theoretical inclusion count remains. After the image analysis, ChlamyCount provides a detailed .txt and .xls output of the 16 areas with the inclusion counts; the total areas above the threshold, and, if confluent, high-intensity areas were detected and could not be dissected to individual inclusions by the software; and the total area/median area ratio is also provided. The median area size is suspected to be the area of an individual inclusion when the MOI is not high, i.e., equal to or below 1. The third output file is a .pdf file with the above-mentioned numerical results and the processed images of the 16 areas (Fig. 2C). A typical scanning time is about 10 min, and the image analysis time is about 1 to 5 min.

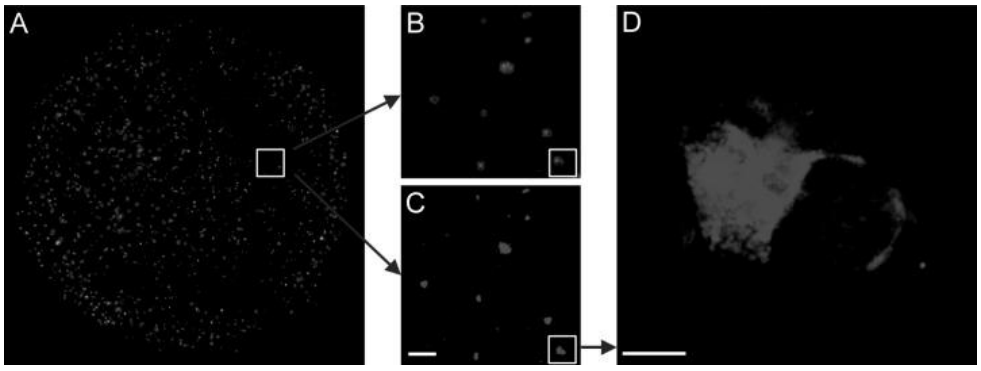

FIG 1 Comparison of the images produced by a DNA chip scanner and confocal microscopy

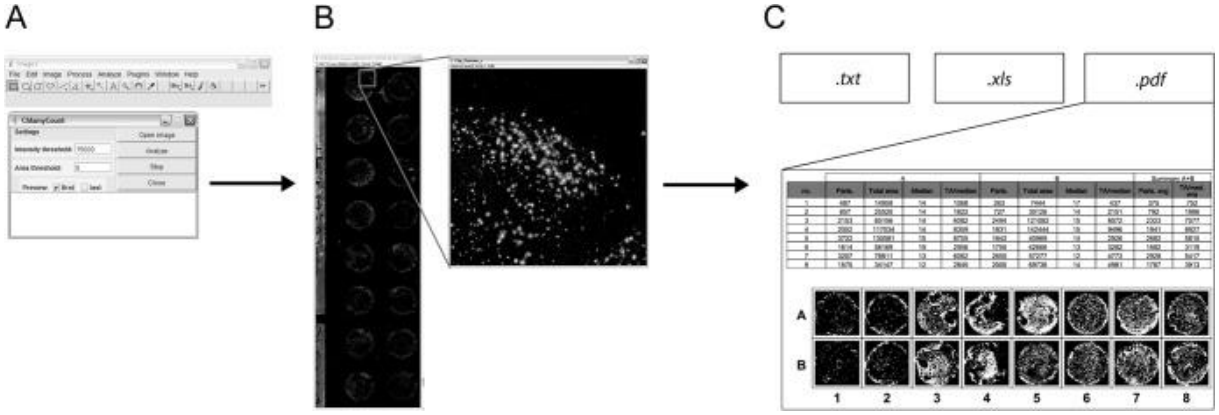

FIG 2 ChlamyCount image adjustments and report

Measuring the dynamic range of detection of *C. trachomatis* serovar D, *C. trachomatis* serovar L2, and *C. pneumoniae*.

The ChlamyCount system was tested on McCoy cells infected with a 1:2 dilution series of *C. trachomatis*serovar D, *C. trachomatis* serovar L2, and *C. pneumoniae*. The *C. trachomatis* serovar D infection was performed using the DEAE-dextran method, the *C. trachomatis* serovar L2 infection was performed without DEAE-dextran, and the *C. pneumoniae* infections were performed by centrifugation (400 × *g*, 60 min, RT). Since both *C. trachomatis* serovars have a faster developmental cycle, the inclusion counting was performed at 24 h p.i., while for *C. pneumoniae* it was performed at

48 h p.i. Initially, the highest MOI was 8, but between MOIs of 8 and 1, the infected areas were highly confluent and ChlamyCount could not dissect these areas efficiently. For further experiments, the starting MOI was either 1 (*C. trachomatis* serovars D and L2) or 1:8 (*C. pneumoniae*), and 6 additional 1:2 dilutions were performed in duplicate. The last two wells contained uninfected McCoy cells (Fig. 3A to C). With all three *Chlamydia* species, we could measure a high correlation (R^2 = 0.95 to 0.98) between the measured *Chlamydia* inclusion count (in the report, particle count) and the theoretical inclusion count calculated from the 1:2 dilution curve. The other two calculated values, namely, the total area above the intensity threshold and the total area/median area ratios, also highly correlated with the calculated theoretical values. When no centrifugation was used for infection (*C. trachomatis* serovars D and L2), the inclusion counts closely followed the theoretical inclusion counts between an MOI of 1 and MOIs of 1:8 to 1:16, resulting in an approximately 1-log-unit dynamic range of the ChlamyCount system. The detected inclusion counts did not change substantially after an MOI of 1:16, marking the lower threshold of detection. The centrifugation was more efficient and permitted us to use lower MOIs for *C. pneumoniae* infection (Fig. 3C); however, we experienced leakage in about 25 to 30% of the chambers; hence, this infection method was not used for other experiments.

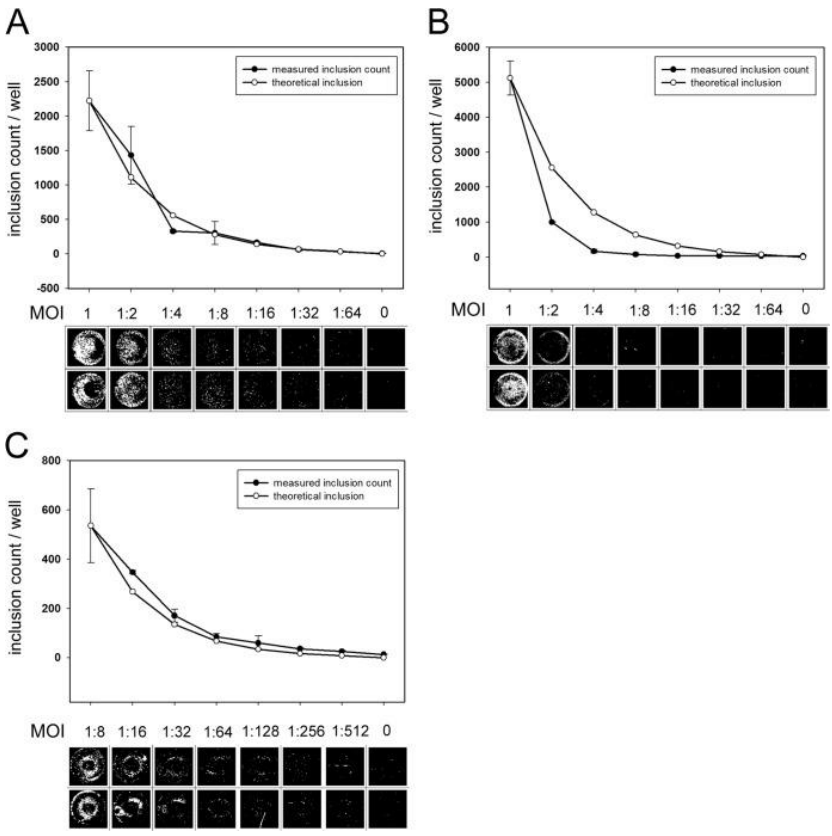

FIG 3 Detection of chlamydial inclusions.

Measuring the MICs of moxifloxacin, tetracycline, and the novel antichlamydial compound PCC00213 for *C. trachomatis* serovar D growth.

We tested whether ChlamyCount was capable of determining the MICs of the known antichlamydial antibiotics moxifloxacin and tetracycline. The *C. trachomatis* serovar D moxifloxacin MIC was

previously characterized to be 0.03 to 0.05 µg/ml (Peuchant et al., 2011). We performed *C. trachomatis* serovar D infections (MOI, 1) in the presence of moxifloxacin at concentrations ranging from 0.25 µg/ml to 0.04 µg/ml. Our experiments showed (Fig. 4A) that *C. trachomatis* could grow in the presence of moxifloxacin up to a concentration of 0.015 µg/ml but was inhibited at a concentration of 0.031 µg/ml, resulting in an MIC value of 0.031 µg/ml. Tetracyclines are first-choice antibiotics for the treatment of chlamydial infections (Mishori et al., 2012). The tetracycline and doxycycline MICs for *C. trachomatis* serovar D were previously characterized to be 0.03 to 0.15 µg/ml (Welsh et al., 1992). We performed *C. trachomatis* serovar D infections (MOI, 1) in the presence of tetracycline at concentrations ranging from 0.04 µg/ml to 0.0006 µg/ml. Our experiments revealed (Fig. 4B) that *C. trachomatis* could grow in the presence of tetracycline up to a concentration of 0.01 µg/ml but was inhibited at a concentration of 0.02 µg/ml, resulting in a MIC value of 0.02 µg/ml. We also used ChlamyCount to determine the MIC of the novel antichlamydial compound PCC00213. As Fig. 4C shows, *C. trachomatis*could grow in the presence of PCC00213 up to a concentration of 3.1 µg/ml but was inhibited at a concentration of 6.2 µg/ml, resulting in a MIC value of 6.2 µg/ml. We have to note that parallel MTT-based host cell viability assays showed that the antichlamydial effect of PCC00213 was partially due to the inhibition of host cell metabolism (data not shown). Parallel to the ChlamyCount-based MIC determination, we investigated the same slides with fluorescence microscopy and determined the inclusion counts in each chamber. As Fig. 4A to C show, the absolute inclusion counts were generally higher when we applied ChlamyCount, but there was a high correlation between the two inclusion counts (R^2 = 0.94 to 0.98) (Fig. 4D). Importantly, the MIC values determined by the ChlamyCount and manual methods were identical for all three tested compounds.

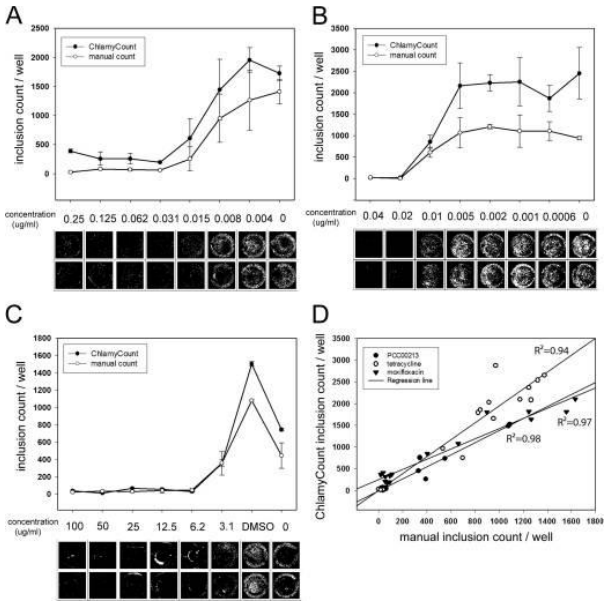

FIG 4 Estimation of MICs of known and novel antimicrobial compounds.

Measuring the effect of IFN-γ on *C. trachomatis* serovar D and DEAE-dextran and cycloheximide on*C. trachomatis* serovar D and *C. pneumoniae* growth.

The inhibitory activity of IFN-γ on chlamydial growth in human host cells via the degradation of the host tryptophan pool is a well-known phenomenon (Byrne et al., 1986). Byrne et al. found that IFN-γ had concentration-dependent inhibitory activity on *C. psittaci* growth in the human uroepithelial cell

line T24, resulting in an approximately 10-fold reduction of direct inclusion counts at a 20-ng/ml IFN-γ concentration. We performed*C. trachomatis* infection (MOI, 1) of McCoy murine fibroblastoid cells in the presence of murine and human IFN-γ. Despite the fact that the host species, cell line, and chlamydial species were different from those used by Byrne et al. (Byrne et al., 1986), our experiments showed a comparable extent of inhibition, albeit at a lower murine IFN-γ concentration: inhibition of chlamydial propagation was concentration dependent, and the maximum inhibition was approximately 3.8-fold at a murine IFN-γ concentration of 1.5 IU/ml (approximately 0.07 ng/ml) or higher (Fig. 5A and and B). The human IFN-γ control did not show any inhibitory effect even at a concentration of 100 IU/ml (Fig. 5A). It was an early observation that the pretreatment of host cells with DEAE-dextran or treatment with cycloheximide could increase the number of chlamydial inclusions and the recoverable number of IFU (Sabet et al., 1984). We applied ChlamyCount to detect these effects during *C. trachomatis* serovar D and *C. pneumoniae* infection. We pretreated HeLa cells with DEAE-dextran (1% DEAE-dextran, 15 min, RT) and/or applied 1 µg/ml cycloheximide during the infection and compared the direct inclusion counts to those for the untreated cells. Our results showed partially different effects of these drugs on the growth of the two *Chlamydia* species (Fig. 5C and andD).D). For *C. trachomatis* serovar D, the application of DEAE-dextran showed only a marginal effect, but the cycloheximide treatment increased the direct inclusion count 1.9- to 2.2-fold largely independently of the presence of DEAE-dextran. For *C. pneumoniae*, the application of dextran or cycloheximide alone increased the direct inclusion count 2.4- and 3.3-fold, respectively, but the coaddition of the two drugs did not show a further growth-promoting effect.

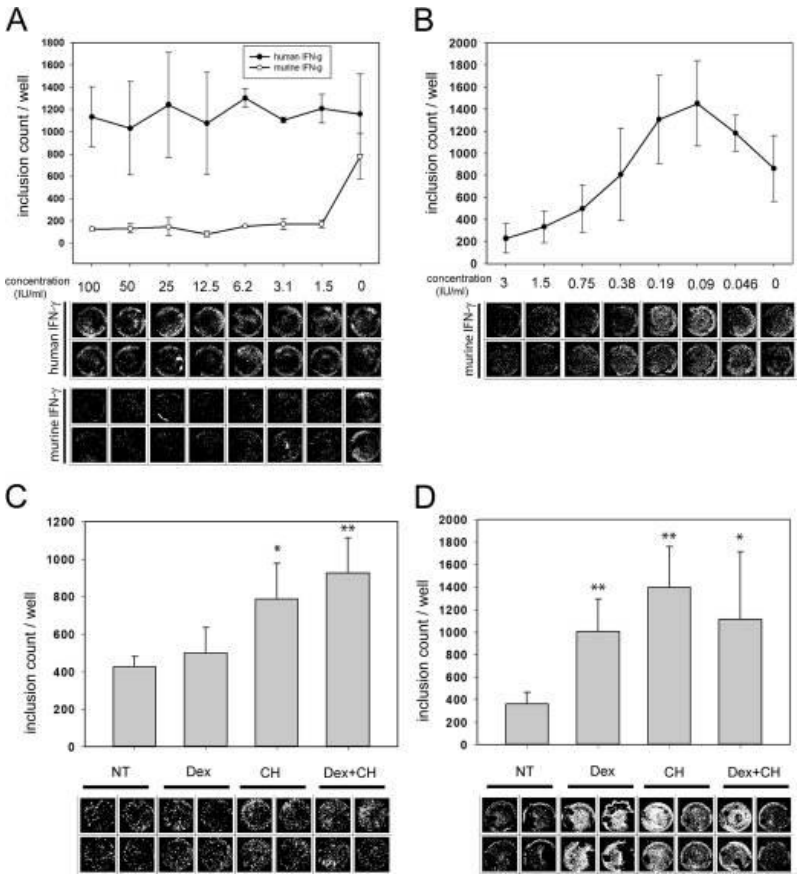

FIG 5 Measuring the effects of IFN-γ, DEAE-dextran, and cycloheximide on the direct inclusion counts of *C. trachomatis* serovar D and *C. pneumoniae*.

In conclusion, we developed an easily useable, accurate system for measuring the antichlamydial effects of known and novel antibiotics and for measuring the effects of various compounds on chlamydial growth. We think that ChlamyCount has the potential to be further optimized. An extended dynamic range of detection and absolute inclusion number estimation may be achieved by applying new raw image-processing methods and an improved confluent area dissection algorithm, goals we are currently pursuing.

VI. TRANSCRIPTION ANALYSIS OF *CHLAMYDIA TRACHOMATIS* D and *HERPES SIMPLEX*-INFECTED HELA CELLS, TÍMEA MOSOLYGÓ[1], EMESE PETRA BALOGH[1], ADRIENN KARAI[1], FANNI KEREKES[1], D. VIRÓK[2] KATALIN BURIÁN[1] manusript in preparation

Chlamydia trachomatis serovars D-K are the most reported sexually transmitted disease (STD) agents associated with urethritis and cervicitis worldwide. The most serious sequelae of C*. trachomatis* infection are: pelvic inflammatory disease (PID), ectopic pregnancy and infertility. These sequelae may have important lifetime consequences and are extremely costly to treat. *Herpes simplex* virus type 2 is an enveloped DNA virus of the viral family Herpesviridae. HSV-2 is the primary cause of genital herpes infection, causing more millions of new infections annually. HSV-2 infection usually occurs on the mucous membranes and skin surrounding the genitals, causing a characteristic ulcerated lesion. After primary infection, HSV-2 can establish a life-long latent infection in the neurons of the sacral ganglia, which is reactivated, on average, 5 times each year. Although most genital HSV infections are clinically mild, HSV-2 can cause serious diseases, including keratitis, meningitis and encephalitis. Several epidemiological studies have shown that *C. trachomatis* and HSV2 co-infection occur in vivo. However, previous studies did not deal with the co-infection process and its molecular biological background in detail. Our aim was to investigate the effect of *Chlamydia trachomatis D* an HSV2 infection on HeLa cells' gene expression.

HeLa cells were infected with *Chlamydia trachomatis D* at a multiplicity of infection of 1 and cultured. After 20 h a part of the cells was superinfected with Herpes simplex virus 2 at a m.o.i. of 1. 24 h after superifection cells were harvested. The recoverable chlamydial titre was determined with indirect immunofluorescent test. The TCID50 titer of the HSV2 was measured on VERO cells Total RNA was extracted from the infected and co-infected cells and non-infected parallel samples. Total RNA integrity was tested by a standard gel analysis. One part of the RNA was subjected to DNA microarray test. Total RNA was amplified using eukaryotic target preparation protocol and hybridized to an Affymetrix whole genome DNA chip. For validation, the same RNA was spared for quantitative polymerase chain reaction analysis that used for DNA chip. The supernatants of the infected cells were also spared for further cytokine chemokine ELISA tests.
HSV2 reduced the chlamydial titer approximately 50 % compare to the *C. trachomatis*-infected control after 48 h incubation. It is interesting that the *C. trachomatis* infection did not influenced the replication of the HSV2, the TCID 50 titer of the co-infected cells were similar to the HSV2-infected control cells.

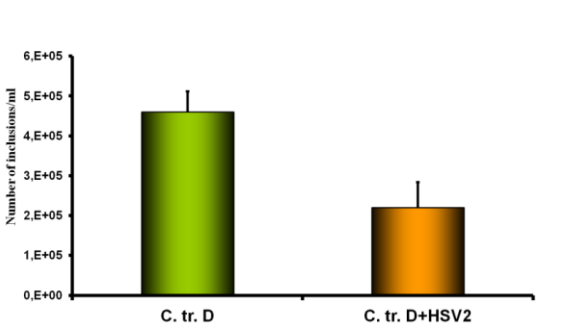

Figure 1: Quantity of the re-coverable *C. trachomatis*

The DNA chip analysis clearly showed that *Chlamydia trachomatis* D serovar and the *Herpes simplex* virus 2 infection has an enhancing effect on the gene expression of the epithelial cells. The *Chlamydia trachomatis* alone and the *Herpes simplex 2* virus infection alone up-regulated the expression of 189 and 95 genes respectively, whereas the combination up-regulated the expression of 151 genes only. The down-regulation pattern was similar. The *C. trachomatis* treatment alone *or Herpes simplex* infection alone down-regulated the expression of 160 and 58 genes, respectively, while the combined treatment repressed 45 genes.

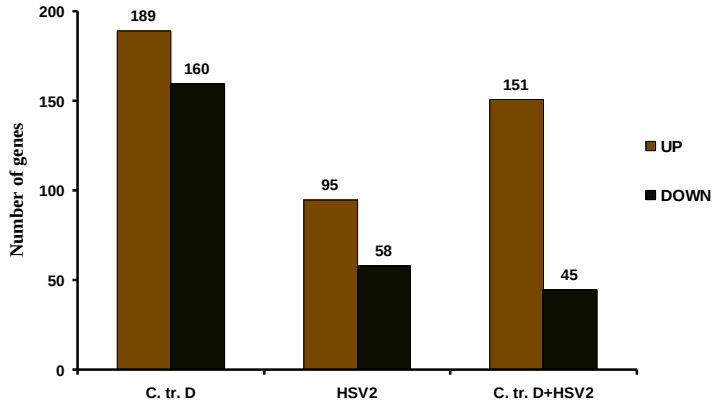

Figure 2: Number of the up or dawn-regulated genes

On the basis of the DAVID Webbased Gene Ontology analysis the altered genes were grouped functionally. Figure 3 shows the name of the functional groups: transcription-, tRNA aminoacylation, translation, antigen processing and presenting, metallothionein-associated genes.

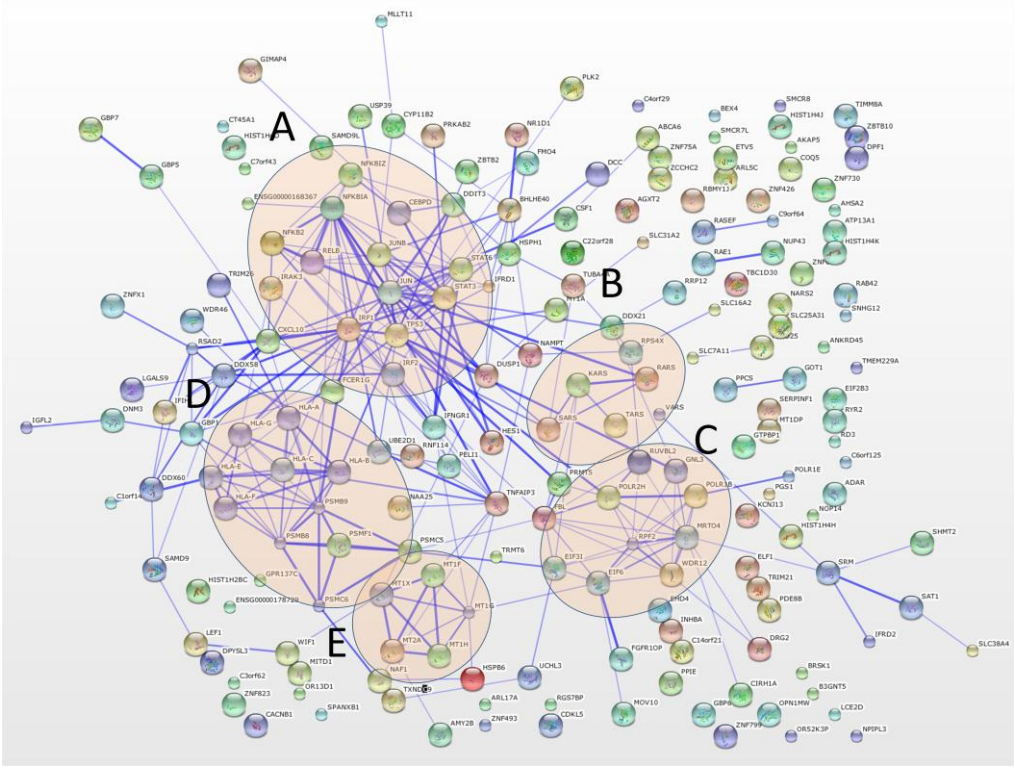

Figure 3. Interaction network analysis of up-regulated genes (http://string-db.org

The expression of the genes related to the **transcription factors** was increased after infection with *C. trachomatis*. The expression was not so marked after HSV2 infection alone. The expression of certain transcription factor genes such as NFκB2, IRF1, TP53, STAT3 and RELB was more pronounced in the case of co-infection. We could detect several transcription factor genes, that could have a role in the Chlamydia-induced inflammation, such as JUNB, JUN, NFKB2, NFKBIZ, NFKBIA, RELB. Several other genes were detected that were involved in the IFN-gamma induced signal transduction cascade, such as IRF1, STAT3 and STAT6. In most of the cases, *Chlamydia trachomatis* infection alone was a potent inducer of transcription factor genes' expression, but the co-infection with the two pathogens didn't have an additive effect

It is known that **STAT3** mediates the expression of variety of genes in response to cell stimuli; ad thus plays a key role in many cellular processes such as cell growth and apoptosis. It is also essential for the differentiation of the TH17 helper T cells. **IRF1** has been shown to play roles in the immune response (regulates the expression of IFNα,ß, p53), regulating apoptosis, DNA damage and tumor suppression. Beyond its function as a transcription factor, IRF-1 has also been shown to transactivate the tumour suppressor protein p53. **P53** is a tumor suppressor protein that in humans is encoded by the TP53 gene. p53 is crucial in multicellular organisms, where it regulates the cell cycle and, thus, functions as a tumor suppressor that is involved in preventing cancer. **NFκB** plays a key role in regulating the immune response to infection. **RELB** belongs to the NFκB/Rel family

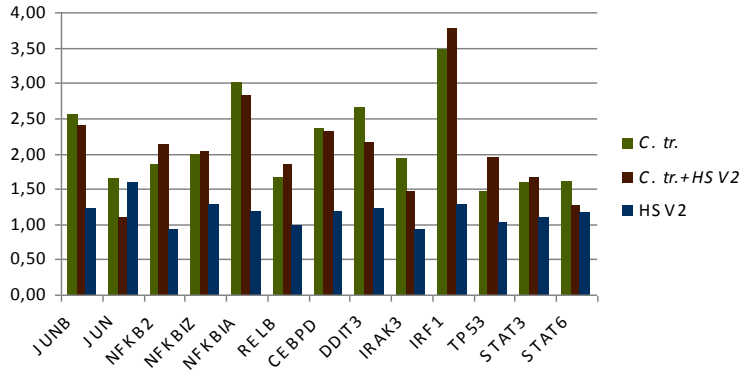

Figure 4. Expression of the genes related to the transcription factors

In point of **tRNA aminoacylation** we can tell that the co-infection has synergistic effect. It is interesting that in the case of co-infection, the expression of the tRNA synthetases were higher. As these enzymes can bind the host cells' aminoacids, chlamydiae are not able to replicate properly. This finding could be the possible explanation for our finding that HSV2 infection can reduce the chlamydial titre by 50%. It is interesting, that the expression of the NARS2 was higher in the case of HSV2 infection.

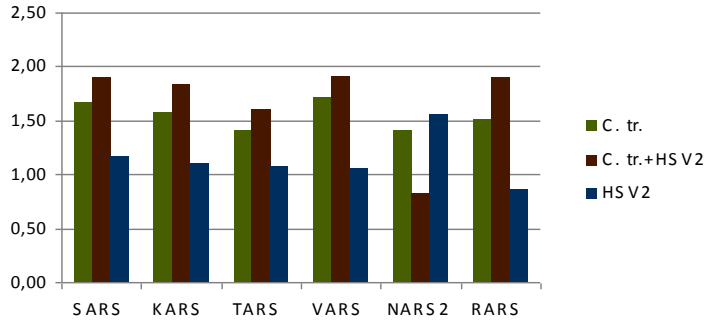

Figure 5. Expression of the genes related to tRNA aminoacylation

As a response to the infection the host cell enhances the protein synthesis. The **translation**-associated genes' expression was increased in the case of *C. trachomatis* D or HSV2 infection alone. The co-infection with the two pathogens caused more marked increase in the gene expression, except for genes RPS4X and RPS26.

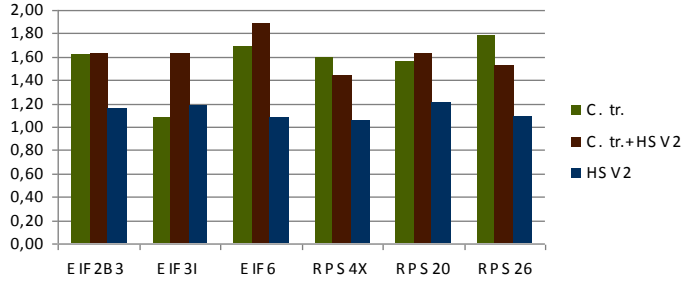

Figure 6. Expression of the translation-related genes

As it can be seen the genes associated with **antigen presentation** are up-regulated after all infection conditions. It seems little bit controversial, because the functional studies described earlier that both *C. trachomatis* and HSV2 are able to decrease the expression of the MHC protein on the cell surface. In that cases the inhibition of the expression of MHC proteins is due to the postranslational process–like inhibition of the TAP protein or degradation of the MHC α chain instead of transcriptional inhibition.

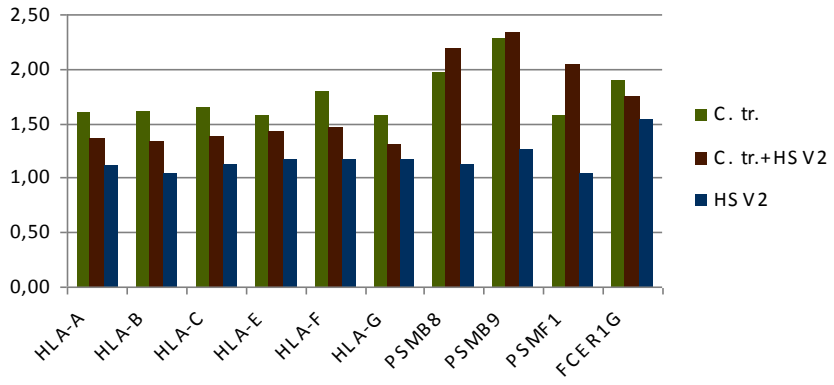

Figure 7. Expression of the genes related to the antigen presentation

Metallothionein is a low-molecular-weight, cysteine-rich, metal binding protein. Although the primary function of metallothioneins is not fully elucidated, experimental data suggest that metallothioneins provide protection against oxidative stress and metal toxicity by binding heavy metals. Metallothioneins play a pivotal role in Zn-related cell homeostasis because of their high affinity for this trace element. By binding and releasing zinc, metallothioneins may regulate zinc levels in the body. Zinc, in turn, is a key element for the activation and binding of certain transcription factors through its participation in the zinc-finger region of the protein. As it can be seen in the figure, *Chlamydia trachomatis* infection enhanced the genes associated with metallothionein proteins. A possible explanation for this finding is that the bacterial infection triggers the formation of ROS, which leads to oxidative stress; on the other hand, the high zinc level can be toxic for Chlamydia.

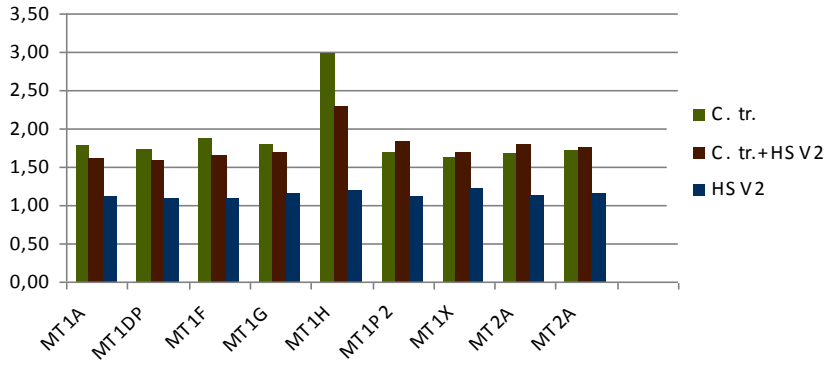

Figure 8. Expression of the metallothionein -related genes

It was an interesting finding that Chlamydia and also HSV2 down-regulated the Wnt signaling pathway, because it is known that the expression of Wnt5 is up-regulated during pathological conditions, involving inflammation.

The HSV2 was able to decrease the number of the recoverable Chlamydiae by 50 %. In contrast with this finding, the *C. trachomatis* did not influence the HSV2 titre. *Chlamydia trachomatis* infection alone has the highest, while HSV2 has the lowest impact on host gene expression. The most interesting finding was that the co-infection of the cells with the two pathogens did not increased the number of the up-regulated genes neither in an additive, nor in a synergistic manner, but decreased it.

References

Brogden, N.K., Brogden, K.A.: Will new generations of modified antimicrobial peptidesimprove their potential as pharmaceuticals? Int J Antimicrob Agents **38**, 217–225 (2011).

Byrne GI, Lehmann LK, Landry GJ. 1986. Induction of tryptophan catabolism is the mechanism for gamma-interferon-mediated inhibition of intracellular Chlamydia psittaci replication in T24 cells. Infect. Immun. 53:347–351

Chen, D., Lei, L., Lu, C., Galaleldeen, A., Hart, P.J., Zhong, G., 2010. Characterizationof Pgp3, a Chlamydia trachomatis plasmid-encoded immunodominant antigen. J. Bacteriol. 192, 6017–6024.

Collins TJ. 2007. ImageJ for microscopy. Biotechniques 43:25–30. 10.2144/000112505

Comanducci, M., Manetti, R., Bini, L., Santucci, A., Pallini, V., Cevenini, R., Sueur, J.M.,Orfila, J., Ratti, G., 1994. Humoral immune response to plasmid protein pgp3 in patients with Chlamydia trachomatis infection. Infect. Immun. 62, 5491–5497.

Gong, S., Yang, Z., Lei, L., Shen, L., Zhong, G., 2013. Characterization of Chlamydia trachomatis plasmid-encoded open reading frames. J. Bacteriol. 195, 3819‑3826.

Hadley, E.B., Hancock, R.E.: Strategies for the discovery and advancement of novelcationic antimicrobial peptides. Curr Top Med Chem **10**, 1872–1881 (2010).

Iwakura Y, Nakae S, Saijo S and Ishigame H: The roles of IL-17A in inflammatory immune responses and host defense against pathogens. Immunol Rev *226*: 57-79, 2008.

Kari, L., Whitmire, W.M., Olivares-Zavaleta, N., Goheen, M.M., Taylor, L.D., Carlson,J.H., Sturdevant, G.L., Lu, C., Bakios, L.E., Randall, L.B., Parnell, M.J., Zhong, G., Caldwell,H.D., 2011. A live-attenuated chlamydial vaccine protects against trachomain nonhuman primates. J. Exp. Med. 208, 2217‑2223

Li, Z., Chen, D., Zhong, Y., Wang, S., Zhong, G., 2008. The chlamydial plasmid-encodedprotein pgp3 is secreted into the cytosol of Chlamydia-infected cells. Infect. Immun. 76, 3415‑3428

Mishori R, McClaskey EL, WinklerPrins VJ. 2012. Chlamydia trachomatis infections: screening, diagnosis, and management. Am. Fam. Physician 86:1127–1132

Mosolygo T, Korcsik J, Balogh EP, Faludi I, Virok DP, Endresz Vand Burian K: *Chlamydophila pneumoniae* re-infection triggers the production of IL-17A and IL-17E, important regulators ofairway inflammation. Inflamm Res *62*: 451-460, 2013.

Nallu, S., Silverstein, K.A., Samac, D.A., Bucciarelli, B., Vance, C.P., VandenBosch, K.A.:Regulatory patterns of a large family of defensin-like genes expressed in nodules of *Medicago truncatula.* PLoS One **8**, e60355 (2013).

O'Neill CE, Seth-Smith HM, Van Der Pol B, Harris SR, Thomson NR, Cutcliffe LT, Clarke IN. 2013.Chlamydia trachomatis clinical isolates identified as tetracycline resistant do not exhibit resistance in vitro: whole-genome

sequencing reveals a mutation in porB but no evidence for tetracycline resistance genes.Microbiology 159(Pt 4):748–756. 10.1099/mic.0.065391-0

Peuchant O, Duvert JP, Clerc M, Raherison S, Bebear C, Bebear CM, de Barbeyrac B. 2011. Effects of antibiotics on Chlamydia trachomatis viability as determined by real-time quantitative PCR. J. Med. Microbiol. 60:508–514. 10.1099/jmm.0.023887-0

Powers, J.P., Hancock, R.E.: The relationship between peptide structure and antibacterialactivity. Peptides **24**, 1681–1691 (2003).

Sabet SF, Simmons J, Caldwell HD. 1984. Enhancement of Chlamydia trachomatis infectious progeny by cultivation of HeLa 229 cells treated with DEAE-dextran and cycloheximide. J. Clin. Microbiol. 20:217–222

Schautteet, K., De Clercq, E., Vanrompay, D.: *Chlamydia trachomatis* vaccine research through the years. Infect Dis Obstet Gynecol **2011**, 963513 (2011).

Shaw, K., Coleman, D., O'Sullivan, M., Stephens, N.: Public health policies and managementstrategies for genital *Chlamydia trachomatis* infection. Risk Manag Healthc Policy **4**,57–65 (2011).

Song, L., Carlson, J.H., Whitmire, W.M., Kari, L., Virtaneva, K., Sturdevant, D.E.,Watkins, H., Zhou, B., Sturdevant, G.L., Porcella, S.F., McClarty, G., Caldwell, H.D.,2013. Chlamydia trachomatis plasmid-encoded Pgp4 is a transcriptional regulator of virulence-associated genes. Infect. Immun. 81, 636‑644.

Thomas, N.S., Lusher, M., Storey, C.C., Clarke, I.N., 1997. Plasmid diversity in Chlamydia.Microbiology 143, 1847‑1854

Tiricz, H., Szucs, A., Farkas, A., Pap, B., Lima, R.M., Maróti, G., Kondorosi, É., Kereszt,A.: Antimicrobial nodule-specific cysteine-rich peptides induce membrane depolarization-associated changes in the transcriptome of *Sinorhizobium meliloti*. Appl EnvironMicrobiol **79**, 6737–6746 (2013).

Welsh LE, Gaydos CA, Quinn TC. 1992. In vitro evaluation of activities of azithromycin, erythromycin, and tetracycline against Chlamydia trachomatis and Chlamydia pneumoniae. Antimicrob. Agents Chemother.36:291–294. 10.1128/AAC.36.2.291